Enhancing superconductivity in bulk β-Bi$_2$Pd by negative pressure induced by quantum electronic stress

Xiaoming Zhang,[1,2,3] Mingwen Zhao,[3] and Feng Liu [2,*]

[1]*Institute for Advanced Study, Tsinghua University, Beijing 100084, China*
[2]*Department of Materials Science and Engineering, University of Utah, Salt Lake City, Utah 84112, USA*
[3]*School of Physics and State Key Laboratory of Crystal Materials, Shandong University, Jinan, Shandong 250100, China*

An effective way to enhance the critical temperature (T_c) of bulk superconductivity (SC) is employing external pressure accompanied with or without phase transitions. However, the variations of T_c are not always "positively" proportional to the pressure even in the same superconducting phase. There exist a class of bulk superconductors such as β-Bi$_2$Pd, whose T_c will be suppressed by pressure starting from the atmospheric pressure. Then the pressure approach of enhancing SC becomes invalid because it is impossible to apply a negative pressure. Here we demonstrate that quantum electronic stress (QES) induced by electronic doping affords a general approach to further enhance T_c of such kinds of bulk superconductors without causing phase transition. Our first-principles calculations show that electron doping gives rise to a negative QES acting as an effective "*negative*" pressure, which expands the lattice of β-Bi$_2$Pd. Consequently, it leads to an increase of electronic density of states at the Fermi level and softening of phonon vibration modes, which in turn enhances the strength of electron-phonon coupling. Conversely, the same concept also explains the experimental reports of pressure and hole-type substitution suppressed SC of bulk β-Bi$_2$Pd, which unifies the effects of pressure and chemical substitution into the same theoretical framework of QES tuning SC. We also envision that surface QES induced by quantum confinement may play an important role in affecting the T_c of epitaxial superconductors, such as the experimentally reported β-Bi$_2$Pd thin films.

I. INTRODUCTION

Ever since the discovery of superconductivity (SC), there has been a constant effort to enhance the superconducting transition temperature (T_c). This has not only directly impacted the practical applications of SC but has also indirectly driven for a better theoretical understanding of the underlying mechanisms. In general T_c has been enhanced in two separate ways. One by discovering new high-T_c superconductors distinctively different from the conventional Bardeen-Cooper-Schrieffer (BCS) SCs of metals [1]. An outstanding representative of this class is cuprates with a recorded T_c being higher than 130 K at atmospheric pressure [2] and a mechanism subjected to long-time debate [3]. The other way is by applying an external field effect, in particular pressure. An appealing example is extremely high-pressurized metallic hydrogen with a theoretically predicted T_c above room temperature [4–7].

For BCS SC, high T_c requires a large electronic density of states (DOS) N_F at the Fermi level, a high phonon frequency ω, and a significant electron-phonon coupling (EPC) λ [8,9]. Phase transition induced by external pressure provided an effective route to enhance SC, such as compressed sulfur [10] as well as compressed hydride of sulfur and lanthanum [11–13]. In the absence of phase transition, external pressure is expected to alter interatomic interactions and redistribute

electronic density of bulk superconductors without changing chemical composition, and hence modify N_F, ω, and λ. Consequently, the variation of T_c under pressure depends on specific superconducting phase [14], such as the pressure enhanced SC in most cuprates [15,16], the dome-like variations in part of iron-based superconductors [17–20] and tungsten ditelluride [21,22], and the pressure suppressed SC in almost all of superconducting metallic elements [23,24] and MgB$_2$ [25], as well as certain unconventional superconductors [26–28]. For the former two classes, one can increase the external pressure to maximize T_c. However, for the pressure suppressed SC with the highest T_c emerging at the atmospheric pressure or a lower pressure, little is known on how to further enhance the T_c of this class of bulk superconductors, because one cannot easily apply a negative hydrostatic pressure to a bulk sample, i.e., decrease the external pressure to negative values experimentally. Given the recent experimental studies of bulk β-Bi$_2$Pd showing that its T_c is linearly suppressed by external pressure with a dT_c/dP coefficient of $-0.25 \sim -0.28$ K/GPa [29,30] and can recover through decompression [31], we herein provide a heuristic answer to this question by demonstrating an enhanced T_c in β-Bi$_2$Pd by a quantum electronic stress (QES) induced effective "*negative*" pressure.

QES (σ^Q) is a nonmechanical form of lattice stress induced purely by the electronic excitation and perturbation [32]. It follows a quantum version of Hooke's law:

$$\sigma^Q = \Xi \Delta n,$$

where $\Xi = \partial\mu/\partial\varepsilon_{ij}$ is the electron deformation potential with $\mu = E_F$ for metal and ε_{ij} is the lattice strain; Δn is the change of electron density. Various effects of QES have been shown already [33–37]. It has been reported that QES can affect the initial stage of epitaxial thin-film growth [34,38], improve the reversible electrochemical reaction for sodium-ion batteries [35], enhance the strength of graphene [39], and even shed light on understanding the graphite-to-diamond phase transition [36,37,40]. One very interesting aspects of QES is that it can be either tensile (positive) or compressive (negative) depending on the sign of Δn, i.e., electron and hole doping will induce a compressive and tensile QES, respectively. This implies that one might be able to apply a compressive QES, an effective "*negative*" pressure, which otherwise cannot be achieved by the means of applying external pressure, to a superconductor like β-Bi$_2$Pd by electron doping so as to enhance its T_c.

Using first-principles calculations, we show that the T_c of bulk β-Bi$_2$Pd can indeed be enhanced by QES through electron doping without causing phase transition. We analyze in detail the dependence of N_F, ω, λ on QES in bulk β-Bi$_2$Pd, which work together to provide a favored outcome of T_c with electron doping. Our approach should be generally applicable to other superconductors, or at least other BCS superconductors, with the T_c being suppressed by the external pressure starting from the atmospheric pressure or a lower pressure. Our result is also useful for understanding the underlying mechanism of external pressure and hole-type substitution suppressed T_c reported experimentally [29,30]. As for an epitaxial thin film of β-Bi$_2$Pd, we believe the surface QES induced by quantum confinement plays an important role in leading to the film-thickness-dependent T_c [41]. It might also shed some light on understanding the possible topological SC (TSC) of a β-Bi$_2$Pd thin film, since only the sample with the highest T_c was observed with the Majorana zero modes (MZMs) in the magnetic vortex cores [41]. An in-plane tensile strain is expected to further improve the T_c of a β-Bi$_2$Pd thin film.

II. METHOD AND COMPUTATIONAL DETAILS

Our calculations were performed employing the QUANTUM ESPRESSO package [42] using the Optimized Norm-Conserving Vanderbilt Pseudopotential [43]. The kinetic energy cutoff for wave functions was set to 40 *Ry* and the exchange-correlation of electrons was treated within the generalized gradient approximation in the form of Perdew-Burke-Ernzerhof [44]. The charge density of bulk β-Bi$_2$Pd was calculated on the uniform **k**-point sampling of $8 \times 8 \times 8$ with the Methfessel-Paxton smearing of 0.02 *Ry*, while the $4 \times 4 \times 4$ **q**-point mesh was used to calculate the dynamical matrix, the phonon frequencies, and the variations of the self-consistent potential within density-functional perturbation theory (DFPT) [45]. The atomic structures of thin film β-Bi$_2$Pd with different thicknesses are fully optimized with **k**-point sampling of $10 \times 10 \times 1$ by employing the Vienna *ab initio* simulation pack [46,47], and a vacuum region of more than 30 Å was set up along the out-of-plane direction to avoid the interactions between neighboring images. The van der Waals (vdW) interaction using the Grimme scheme

is taken into account except where noted, but the spin-orbit coupling is ignored due to its negligible effect on the T_c of bulk β-Bi$_2$Pd [48].

The superconducting properties are evaluated by self-consistently solving the fully anisotropic Migdal-Eliashberg formalisms [49–51] based on DFPT and maximally localized Wannier functions (MLWFs) [52], as implemented in the Electron-Phonon Wannier (EPW) code [53]. The electronic wave functions required for the Wannier interpolation within EPW are calculated on a uniform **k**-point mesh same as that of previous charge density calculations. MLWFs were established by using $6p$ orbitals of Bi atom and $4d$ orbitals of Pd atom as an initial guess for the unitary transformations via the WANNIER90 code [54]. The numerical solution of Migdal-Eliashberg equations was performed on a dense electron and phonon mesh of 40^3 sampled in the first Brillouin zone (BZ) of bulk β-Bi$_2$Pd. The Matsubara frequency is truncated at about six times the largest phonon energy, and the screened Coulomb interaction parameter μ^* is set to 0.1. The Dirac δ functions are replaced by Lorentzians with the width of 25 and 0.05 meV for electrons and phonons, respectively.

III. RESULTS

The stoichiometric compound β-Bi$_2$Pd crystallizes into a centrosymmetric body-centered-tetragonal structure (space group *I4/mmm*, No. 139) with the Bi-Pd-Bi layer stacking in an ABA sequence along c direction [Fig. 1(a)]. The experimental lattice constants are $a_0 = 3.362$ and $c_0 = 12.983$ Å [55]. The primitive cell of bulk β-Bi$_2$Pd is constructed by two Bi and one Pd atoms and possesses a rhombohedral structure, as shown in the right panel of Fig. 1(a). After fully optimizing the crystal structure of β-Bi$_2$Pd, the calculated total stress vanishes and the lattice constants are very close to the experimental values, corresponding to the equilibrium state of intrinsic β-Bi$_2$Pd. Previous work reported such equilibrium could be destroyed purely by electronic excitation and perturbation in the absence of lattice strain, and the induced stress is regarded as QES (s^Q) [32]. Figure 1(c) shows the calculated QES as a function of the variation of electron density (Δn) for the charged β-Bi$_2$Pd, simulated by adding (removing) electrons to (from) intrinsic β-Bi$_2$Pd and introducing the compensating jellium background to remove divergence. One can easily identify the linear dependence that can be described by the so-called quantum Hooke's law of $\sigma^Q = \Xi \times \Delta n$. Here the negative (positive) value represents compressive (tensile) QES, which naturally gives rise to nonzero internal pressure [Fig. 1(c)]. The higher the doping concentration, the larger the pressure will be. To eliminate the QES, we further fully optimized the atomic position and the lattice constant of 0.05 hole-doped and 0.05 electron-doped β-Bi$_2$Pd. The volume of primitive cell increases with the increase of electron doping concentration, while the reverse is true for hole doping [Fig. 1(d)]. This demonstrates that QES has a similar effect as external pressure [56], albeit truly negative pressure cannot be experimentally realized otherwise. Thus, QES should provide a promising way of enhancing the SC of bulk β-Bi$_2$Pd by applying an effective "*negative*" pressure because a positive pressure would decrease the T_c [29,30].
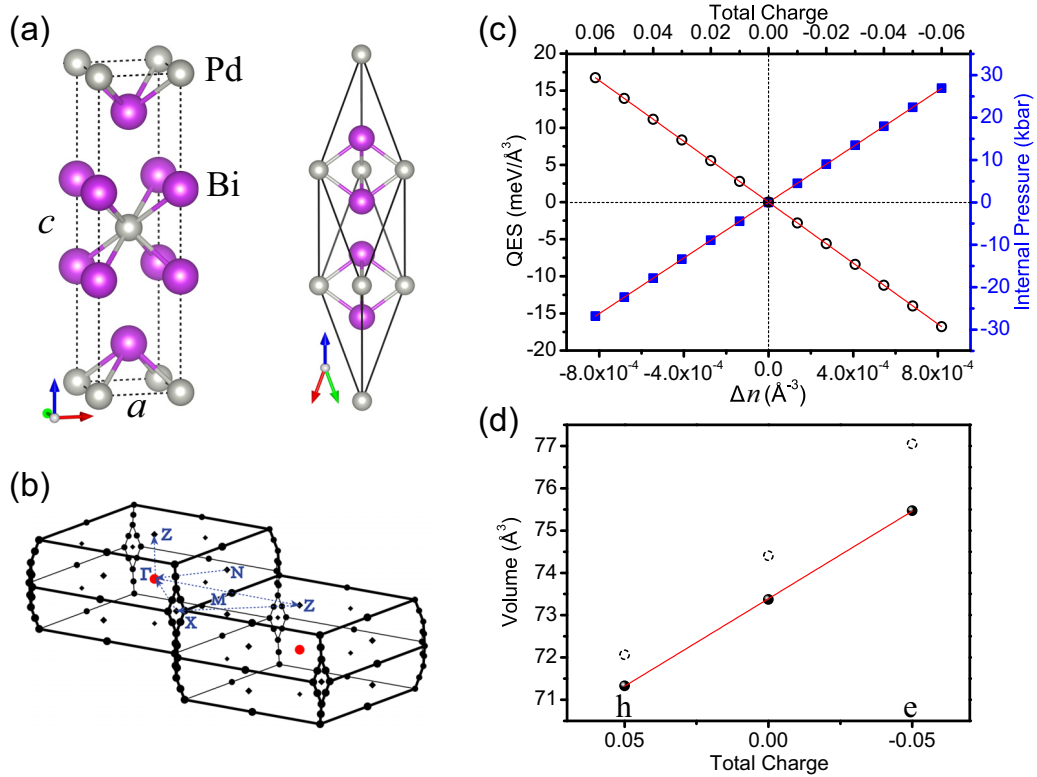
FIG. 1. (a) The crystal structure of bulk β-Bi$_2$Pd represented by conventional unit cell and primitive cell. (b) The BZ for the primitive cell of bulk β-Bi$_2$Pd and the high-symmetry directions for band calculations. (c) The QES and internal pressure as a function of carrier density Δn. (d) The volume of 0.05 hole-doped, intrinsic, and 0.05 electron-doped β-Bi$_2$Pd per primitive cell. The dotted line circles are the data calculated without considering the vdW interaction. The total charge represents the charge of the primitive cell after carrier doping without considering the compensating jellium charges. Red lines are linear fits to the corresponding data. The mark of h/e represents hole/electron doping.

Figure 1(b) presents the BZ of the primitive cell and the relevant high-symmetry directions for band calculations. The calculated electronic band structures of bulk β-Bi$_2$Pd without and with carrier doping are plotted in Fig. 2(a) for
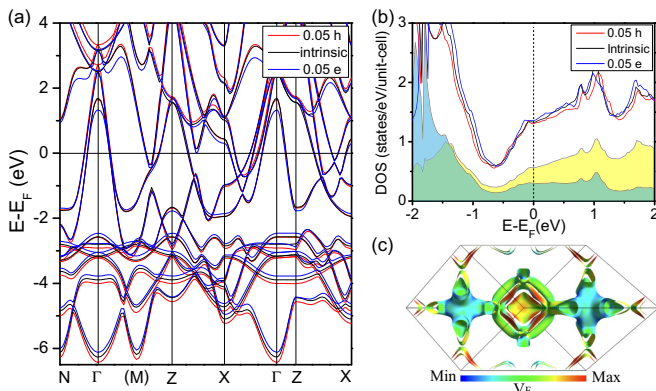

FIG. 2. The comparison of (a) electronic band structure and (b) total DOS for 0.05 hole-doped (red lines), intrinsic (black lines), and 0.05 electron-doped (blue lines) β-Bi$_2$Pd. The yellow and the blue regions represent the projected DOS contributed by the $6p$ orbitals of Bi and $4d$ orbitals of Pd, respectively. (c) The Fermi surface of bulk β-Bi$_2$Pd together with momentum-resolved Fermi velocity (V_F) represented by color.

comparison. One can see the robust metallic property as the bands always intersect with the Fermi level. The similar band dispersions among them indicate that the present doping concentrations do not cause phase transition. Overall, the width of the metallic bands increases with the hole doping, while the reverse is true for electron doping. Such variation can be understood from the perspective of tight-binding theory. Since the electron/hole doping expanding/contracting the volume of bulk β-Bi$_2$Pd [Fig. 1(d)], the increased/decreased interatom distance will reduce/enhance the electron hopping to decrease/increase band width. Such variations in turn modify the electronic DOS and the value of N_F, as shown in Fig. 2(b). Our calculated value of N_F is 1.304, 1.331, and 1.360 states/eV/unit-cell for 0.05 hole-doped, intrinsic, and 0.05 electron-doped β-Bi$_2$Pd, respectively. Thus, N_F increases with the increase of electron density ($N_F \propto \Delta n$). By plotting the projected DOS in Fig. 2(b), we find that the $6p$ orbitals of Bi atoms contribute more states than the $4d$ orbitals of Pd atoms near the Fermi level, indicating the Fermi surface (FS) is mainly constructed by the electronic states of Bi atoms. The FS [Fig. 2(c)] possesses the feature of multiple sheets [48,57,58], which remain almost unchanged in response to carrier doping. The momentum-distributed Fermi velocity (V_F) is also presented in Fig. 2(c). In general, a small Fermi velocity is favorable for strong EPC or a large superconducting gap. Our calculated Fermi velocity is
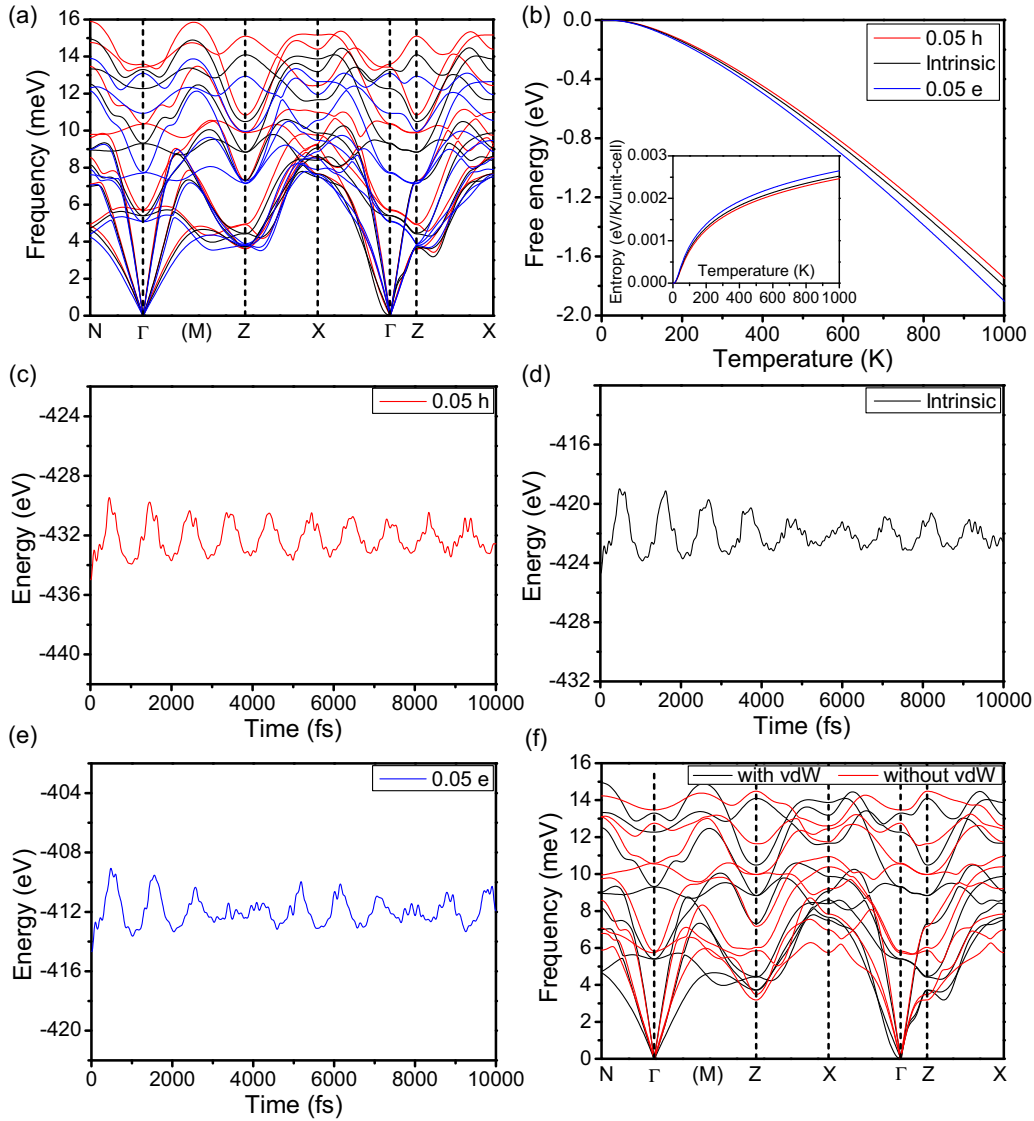
FIG. 3. (a) The phonon spectra, and (b) the free energy F as well as entropy S of 0.05 hole-doped (red lines), intrinsic (black lines), and 0.05 electron-doped (blue lines) β-Bi$_2$Pd. The free energies were calculated without considering the zero-point energy and the contribution of electron thermal excitation. The entropies were calculated by $S = -dF/dT$. The total energy fluctuations of (c) 0.05 hole-doped, (d) intrinsic, and (e) 0.05 electron-doped β-Bi$_2$Pd with respect to the molecular dynamics simulation time at 300 K using a $3 \times 3 \times 3$ supercell. (f) The comparison of the phonon spectra calculated with and without considering vdW interaction for intrinsic β-Bi$_2$Pd.

consistent with the momentum-resolved superconducting gap $\Delta_{\mathbf{k}}$ reported previously [48].

Since the electronic states near the Fermi level are well delocalized and contributed mainly by the $6p$ orbitals of Bi atom [Fig. 2(b)], the electron correlation effect is expected to be small and hence neglected. Meanwhile, the delocalized states lead the electronic entropy to be a small quantity with respect to the entropy contributed by phonons, because only the electrons with the energy difference of $\sim k_{\mathrm{B}}T$ to the Fermi level participate in the thermal excitations. Electronic entropy can be calculated based on the equation of

$$S_e(T) = - \int N(\varepsilon, T)\{f(\varepsilon, T) \ln f(\varepsilon, T)$$
$$+ [1 - f(\varepsilon, T)] \ln[1 - f(\varepsilon, T)]\}d\varepsilon,$$

where $N(\varepsilon, T)$ and $f(\varepsilon, T)$ are the temperature-dependent density of states and Fermi distribution function, respectively. If we assume the $N(\varepsilon, T)$ and $f(\varepsilon, T)$ are temperature-independent, the electronic entropy shows a linear dependence with density of states at the Fermi level: $S_e = \frac{\pi^2}{3} k_B^2 T N_F$, which provides an accurate approximation around room temperature for the systems with delocalized states [59]. Consequently, electronic entropy is expected to be slightly increased/decreased by electron/hole-doping.

The phonon spectra of 0.05 hole-doped, intrinsic, and 0.05 electron-doped β-Bi$_2$Pd are plotted in Fig. 3(a). One can confirm the dynamic stability of the carrier doped β-Bi$_2$Pd by the absence of imaginary frequency. With the doping type changing from hole to electron, all the phonon modes tend to be softened gradually. This tendency is also attributed to the enlarged volume of β-Bi$_2$Pd [Fig. 1(d)], which decreases
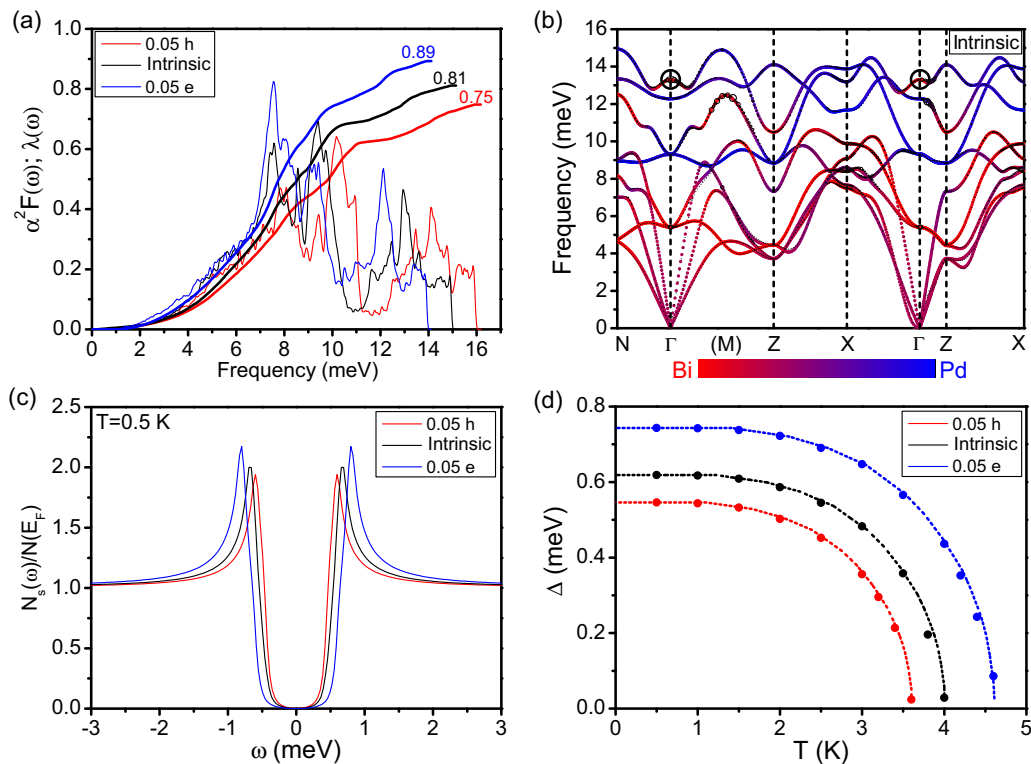
FIG. 4. (a) The Eliashberg spectral function $\alpha^2 F(\omega)$ and cumulative EPC strength $\lambda(\omega)$ of 0.05 hole-doped, intrinsic, and 0.05 electron-doped β-Bi$_2$Pd. (b) The decomposed phonon spectra of intrinsic β-Bi$_2$Pd with the vibration modes of Bi and Pd being indicated by red and blue colors. The black circle is drawn proportional to the magnitude of phonon linewidth $\Pi''_{\mathbf{q}v}$. (c) The normalized quasiparticle DOSs at 0.5 K and (d) the temperature dependent average value of superconducting gap for the β-Bi$_2$Pd considered. The dashed lines in (d) are a guide for the eyes.

interatomic interaction. The effect of scattering channels on modifying the phonon frequency [60,61] is negligible due to the unchanged multiple-sheet FS [Fig. 2(c)]. Hence, no Kohn anomaly is induced [62]. Similar to the electronic band structures, the qualitatively same phonon dispersions indicate that the phase of bulk β-Bi$_2$Pd is well preserved under the doping concentrations considered. Free energy and entropy calculations based on phonon density of states under the quasi-harmonic approximation indicate that the electron doping is more feasible than hole doping [Fig. 3(b)], which is consistent with the recent experimental report of the upward shifted Fermi level in β-Bi$_2$Pd thin film [63]. The thermodynamical stability of β-Bi$_2$Pd at finite-temperature was checked by molecular dynamics simulations using the *NVT* ensemble at 300 K [Figs. 3(c), 3(d), and 3(e)]. One can clearly see the total energies are well converged for 0.05 hole/electron-doped and intrinsic β-Bi$_2$Pd. We also calculated the phonon spectra of intrinsic β-Bi$_2$Pd without considering vdW corrections. The maximum frequency is slightly decreased with respect to that with vdW corrections [Fig. 3(f)], attributed to the structural expansion after ignoring vdW interaction [Fig. 1(d)]. Despite this, the variations of volume per primitive cell with and without considering vdW interaction show a very similar trend in response to the carrier doping [Fig. 1(d)], which indicates that our results and conclusions are unchanged using either method.

Figure 4(a) shows the calculated Eliashberg spectral function $\alpha^2 F(\omega)$ and cumulative EPC strength $\lambda(\omega)$, which indi-

cate that all phonon modes participate in the renormalization of the electron mass. From the cumulative EPC strength, we can clearly see the modes with the frequency lower than ~ 10 meV contribute mainly ($\sim 80\%$) to the total EPC. The decompositions of phonon spectra [Fig. 4(b)] shows that the low-frequency modes stem mainly from the vibrations of the Bi atom, while the vibrations of Pd atoms occupy the high frequency range. Together with the $\mathbf{q}$- and v-resolved phonon linewidth $\Pi''_{\mathbf{q}v}$ [Fig. 4(b)], we conclude that the electrons mainly couple with the vibrations of the Bi atom. This is reasonable since the FSs are mostly constructed by the $6p$ orbitals of Bi atoms (Fig. 2). The values of the total EPC obtained from our calculations are $\lambda = 0.75$, 0.81, and 0.89 for 0.05 hole-doped, intrinsic, and 0.05 electron-doped β-Bi$_2$Pd, respectively. This indicates that electron doping is favorable for enhancing the strength of the EPC.

We then calculated the normalized quasiparticle DOSs in the superconducting state of β-Bi$_2$Pd according to $\frac{N_S(\omega)}{N_F} = $ Re$[\frac{\omega}{\sqrt{\omega^2 - \Delta^2(\omega)}}]$ [51], which can be used to compare with the experimental tunneling conductance directly. The results obtained with the screened Coulomb interaction parameter $\mu^* = 0.1$ at 0.5 K are shown in Fig. 4(c). Both the intrinsic and doped β-Bi$_2$Pd present a pair of van Hove singularities that correspond to a single superconducting gap. Notably, the van Hove singularity gradually moves to the high-energy range when the doping type changes from hole to electron, indicating a tunable superconducting gap for bulk β-Bi$_2$Pd.
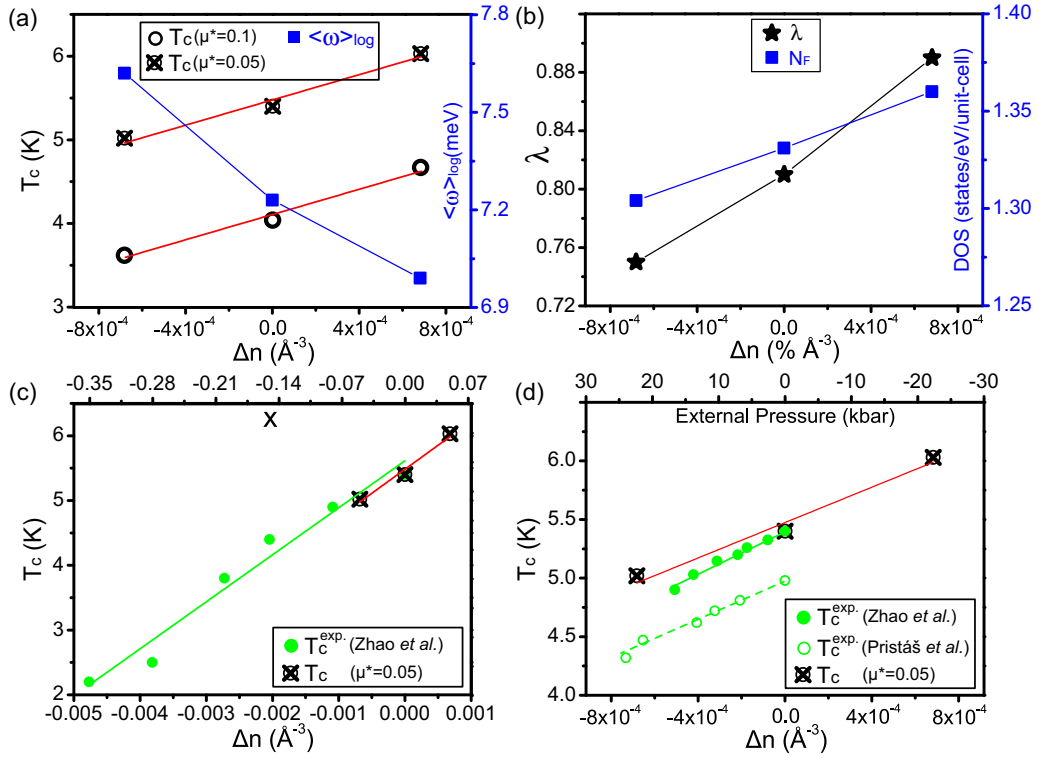
FIG. 5. Summary of (a) the critical temperature T_c estimated by $\mu^* = 0.1$ and 0.05, logarithmically averaged frequency $\langle\omega\rangle_{\log}$, (b) EPC λ, and N_F versus the variation of carrier density Δn. The experimental values of superconducting transition temperature ($T_c^{\text{exp.}}$) of (c) β-Bi$_{2-x}$Pb$_x$Pd and of (d) β-Bi$_2$Pd under external pressures reported by Zhao *et al.* [29] (green dots) and G. Pristáš *et al.* [30] (green open circles) are plotted as the function of carrier density Δn. Red and green lines are linear fits to the corresponding data. The data of T_c estimated by $\mu^* = 0.05$ are replotted in (c) and (d) for comparison.

The T_c of intrinsic β-Bi$_2$Pd is estimated as ~4.04 K, at which the gap vanishes [Fig. 4(d)]. The single superconducting gap of intrinsic β-Bi$_2$Pd is consistent with the previous reports, and the value of T_c is close to the lower limit of the reported experimental values ranging from 4.25 to 5.4 K [55,64,65]. Comparing with the $T_c = 4.40$ K reported by a previous theoretical study [48], we suspect the underestimated critical temperature may be partly attributed to the computational details, such as the **k/q** meshs for numerical solution of the Migdal-Eliashberg equations [51]. Moreover, the uncertain dimensionless Coulomb interaction parameter μ^* (we use $\mu^* = 0.1$ here) should be another reason for the underestimated T_c, and it is well known that a smaller μ^* is favorable for higher T_c. Despite the slight underestimation in the absolute value of T_c with respect to the previous reports, the focus of the present study is the changes of T_c upon doping induced QES, which are importantly reliable.

From Fig. 4(d), one sees that the T_c can be increased to 4.67 K by doping 0.05 electron per primitive cell, while doping 0.05 hole decreases the T_c to 3.62 K. We summarized the calculated data and replotted them in Fig. 5(a). Through linear fitting, a linear enhancement rate of $d(T_c)/d(\Delta n) = 7.7$ K is obtained, which points to a promising perspective of further improving the critical temperature through purely electron-doping-induced lattice expansion. To understand the underlying mechanism of the tunable T_c, we recall the McMillan-Allen-Dynes formula, $T_c = \frac{\langle\omega\rangle_{\log}}{1.2} \exp[\frac{-1.04\times(1+\lambda)}{\lambda-\mu^*\times(1+0.62\times\lambda)}]$ [8,9]. Using the same Coulomb interaction parameter μ^*, a large

logarithmically averaged frequency ($\langle\omega\rangle_{\log}$) and strong EPC λ are beneficial to the condensation into the superconducting state below high critical temperature. The reliability of this formula in estimating the pressure dependence of T_c had already been demonstrated [66–68]. The values of $\langle\omega\rangle_{\log}$ are plotted in Fig. 5(a), which shows the same trend as the aforementioned variations of phonon frequency [Fig. 3(a)]. The trend, however, is opposite to the variation of critical temperature, indicating that the tunable critical temperature cannot be explained alone by $\langle\omega\rangle_{\log}$. This in turn illustrates that the EPC λ plays a key role in tuning the T_c of bulk β-Bi$_2$Pd [Fig. 5(b)]. According to the simplified relation of $\lambda \propto N_F/\omega^2$, the increased λ for 0.05 electron-doped β-Bi$_2$Pd stems from the increased N_F [Fig. 2(b)] and decreased phonon frequency [Fig. 3(a)], triggered by the QES induced structural expansion.

We emphasize here that the structural contraction/expansion induced by QES is essential in tuning the SC of bulk β-Bi$_2$Pd, which magnifies the variations of bandwidth, N_F, and the magnitude of phonon frequency. If we neglect the QES, the change in the dispersion of electron and phonon band structures will be very small due to the absence of structural relaxation. Taking the 0.05 electron-doped β-Bi$_2$Pd as an example, the doped electron slightly moves up the Fermi level, as shown in Fig. 6(a). Despite the positive slope of the DOS, the shift of the Fermi level is too small to induce a visible increase in N_F and visible variations of FS. Together with the unchanged atomic structure, the robust FS
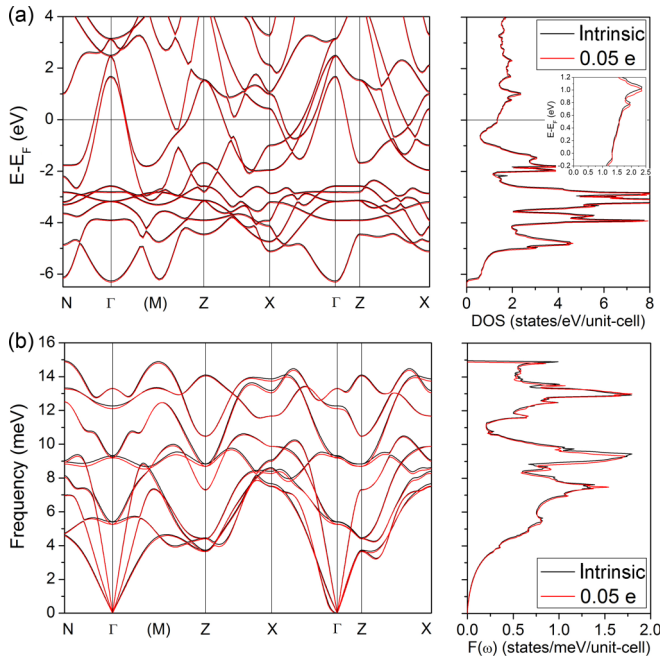
FIG. 6. The band structure and DOSs of (a) electrons and (b) phonons. Black and red lines represent the data of intrinsic and 0.05 electron-doped β-Bi$_2$Pd with the same crystal structure among them. A close-up view is plotted in the inset of (a) to show the shift of the Fermi level clearly.

would yield identical scattering channels among the intrinsic and doped β-Bi$_2$Pd, leading to no obvious change in the phonon spectra and phonon DOS [Fig. 6(b)]. These features indicate that without considering the QES-induced structural expansion, the T_c of the 0.05 electron-doped β-Bi$_2$Pd would be basically the same as that of the intrinsic β-Bi$_2$Pd.

With the parameters of McMillan-Allen-Dynes formula in hand, we try to match the experimental values of T_c by tuning the dimensionless Coulomb interaction parameter μ^*, due to the underestimated T_c with $\mu^* = 0.1$ mentioned above. We found that T_c can reach the experimental value of ~ 5.4 K for intrinsic β-Bi$_2$Pd with $\mu^* = 0.05$. Correspondingly, the values of T_c for carrier doped ones are increased. The above mentioned linear enhancement rate of $d(T_c)/d(\Delta n)$ remains robust [Fig. 5(a)]. We note that $\mu^* = 0.05$ is smaller than the widely used values of $0.1 \sim 0.2$ [51]. It is known that these values cannot always reproduce experimental results. One example is boron-doped diamond, where only the supercell model with $\mu^* \sim 0.067$ could match the superconducting transition temperature of ~ 4 K [69,70]. Here the Coulomb interaction parameter μ^* was estimated by solving simultaneously the equations of McMillan-Allen-Dynes formula. This is done by using the quantities of $T_c = 4$ K and $\lambda = 0.336$ for the supercell model as well as $T_c = 0.3$ K and $\lambda = 0.237$ for the virtual crystal model reported by Giustino *et al.* [70], and assuming the same $\langle \omega \rangle_{\log}$ for the two cases.

IV. DISCUSSION

We emphasize that the QES is induced purely by electronic excitation and perturbation without changing atoms,

which is different from chemical intercalation. The addition of dopants can be regarded as a structural phase transition, where the electronic band structures and phonon spectra are dramatically modified, such as the intercalated transition metal dichalcogenides [71] and graphite intercalated compounds [72]. This may be the reason for the experimental observations of suppressing SC in Na-doped β-Bi$_2$Pd, although the authors attributed it to the emergence of possible spin excitation [29]. On the other hand, chemical substitution without causing a structural phase transition provides a practical way of realizing "electron/hole doping". For example, the hole-doped β-Bi$_2$Pd with Bi substituted by Pb atoms, namely β-Bi$_{2-x}$Pb$_x$Pd, [29] shows the same tendency as our predictions. According to one Pb atom introducing one hole in bulk β-Bi$_2$Pd, we estimated the variations of carrier density by $\Delta n = -x/V_0$. Here $V_0 = 73.37$ Å^3 is the volume per primitive cell of intrinsic β-Bi$_2$Pd. The experimentally reported $T_c^{\text{exp}\cdot}$ of β-Bi$_{2-x}$Pb$_x$Pd versus Δn are summarized in Fig. 5(c). Through linear fitting (green line), a linear enhancement rate of $d(T_c)/d(\Delta n) = 7.6$ K is obtained, which is basically equal to our calculations with the consideration of carrier doping induced QES. Consequently, the hole-type substitution suppressed SC could be understood by the picture of QES induced structural contraction. To confirm our prediction and realize the goal of enhancing the SC in bulk β-Bi$_2$Pd experimentally, we suggest experiments substituting Bi or Pd atoms with the elements having more valence electrons and/or having a larger atomic radius to induce lattice expansion under the premise of avoiding structural phase transition, rather than chemical intercalation.

The QES induced tunable SC of bulk β-Bi$_2$Pd not only provides a promising route towards improving T_c by electron doping or chemical substitution, but also is useful for understanding the previous experimental reports of external pressure suppressed SC [29,30]. From Fig. 1(c), we learn that 0.05 electron/hole doping will give rise to the internal pressure of about $+/-22.34$ kbar via the compressive/tensile QES. Since we have eliminated the QES through fully optimizing the atomic structure, the 0.05 electron/hole-doped β-Bi$_2$Pd can be approximately regarded as the counterpart of intrinsic β-Bi$_2$Pd with an effective pressure of $-/+22.34$ kbar. Consequently, the linear enhancement rate of $d(T_c)/d(\Delta n) = 7.7$ K induced by carrier doping can be translated to $d(T_c)/d(p) = -0.24$ K/GPa, close to the experimental value of $-0.25 \sim -0.28$ K/GPa [29,30], as shown by the almost parallel red and green lines in Fig. 5(d). This consistency stems from the similar effects [56] of internal and external pressure on the volume of bulk β-Bi$_2$Pd, both of which can be linear fitted together [Fig. 7(a)]. Figures 7(b) and 7(c) plot the comparison of band structure and DOS of bulk β-Bi$_2$Pd under the numerically simulated external pressure of $+/-15$ kbar. One can easily identify the same features as those shown in Figs. 2(a) and 2(b), and the N_F of the pressured and carrier doped β-Bi$_2$Pd follow the same trend that can be fitted by the same line [Fig. 7(d)]. Consequently, the pressure suppressed SC can be understood by the increase of logarithmically averaged frequency [Fig. 5(a)] and the decrease of EPC [Fig. 5(b)] based on our above QES analysis, which is qualitatively consistent with a previous report based on fitting the pressure and temperature dependences of normal-state electrical resistivity
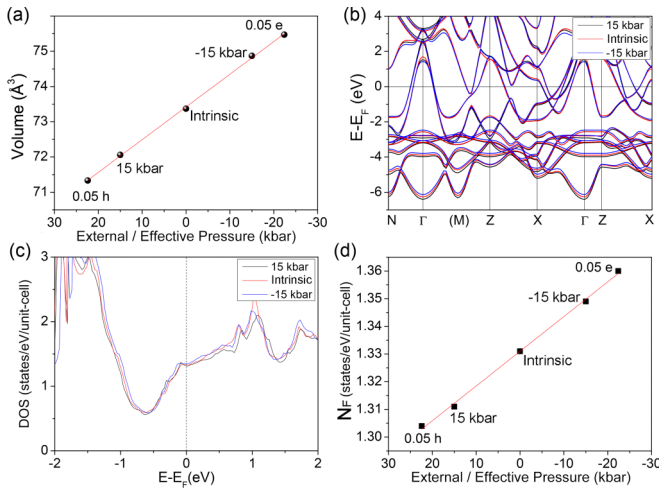
FIG. 7. (a) The plot of volume as a function of external/effective pressure. (b) The band structures and (c) the total DOS of β-Bi$_2$Pd under the numerically simulated external pressure of 15 (black lines), 0 (intrinsic, red lines), and -15 (blue lines) kbar. (d) The linear fit of N_F versus external/effective pressure.
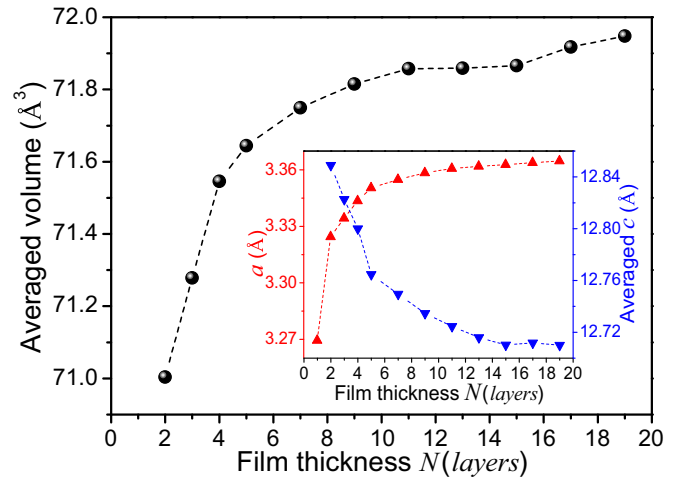

FIG. 8. The averaged volume per chemical formula of Bi$_2$Pd and lattice constant (a) and (c) labeled in Fig. 1(a) versus the film thickness N of β-Bi$_2$Pd thin film. Here the unit of N is the number of Bi-Pd-Bi layers. Please note the different unit of film thickness d used by Lv *et al.* [41] when plotting the film-thickness-dependent T_c.

using simplified Bloch-Grüneisen formula [30]. This indicates the QES indeed plays the same role as external pressure but is more superior, because the electron doping could induce an effective "*negative*" pressure that cannot be realized otherwise by the method of applying external pressure experimentally, and hence can further improve the superconducting transition temperature of bulk β-Bi$_2$Pd.

As for the epitaxial β-Bi$_2$Pd thin film grown on SrTiO$_3$(001), we argue that the lattice expansion/contraction should be one of the possible reasons to induce the film-thickness-dependent T_c [41], in addition to the topological surface states (TSSs) [73]. The lattice expansion/contraction has two origins [32]. One comes from the lattice mismatch between β-Bi$_2$Pd and substrates, given the larger lattice constant ($\sim$3.9 Å) of SrTiO$_3$(001) [74] than that ($\sim$3.362 Å) of bulk β-Bi$_2$Pd [55], which corresponds to conventionally mechanical surface stress. The other is surface QES, which might arise at the initial stage of epitaxial thin film growth due to quantum confinement [34,38]. One can clearly see from Fig. 8 that the average volume per chemical formula of Bi$_2$Pd gradually expands with the increase of film thickness N, which is attributed mainly to the increased in-plane lattice constant a (inset of Fig. 8). The value of a reaches the bulk value of $\sim$3.362 Å at the thickness of $N = 13$ *layers*, which is consistent with a previous report that the well localized TSSs can be observed at the thickness of more than 11 *layers* [58]. Notably, the same variation tendency between the averaged volume and the experimentally reported T_c [41] with respect to the film thickness indeed indicates a positive relationship among them. This correlation provides important information for understanding the origin of film-thickness-dependent T_c for β-Bi$_2$Pd thin film, same as the 111-type iron pnictide superconductors [18]. Additionally, the effect of electron-doping induced QES on the SC of a β-Bi$_2$Pd thin film cannot be negligible since the chemical potential was reported to shift upward about 37 meV with respect to that of bulk β-Bi$_2$Pd recently [63]. The T_c of the β-Bi$_2$Pd thin film is expected to be further improved by applying an in-plane tensile strain, given that the dependence of T_c on lattice strain had already been demonstrated in MgB$_2$ [75]. Moreover, considering the potential TSC of the β-Bi$_2$Pd thin film [64,73,76], the structural expansion/contraction tuned SC may shed some light on understanding the absence and presence of MZMs reported previously [41,65,77,78], since the MZMs were only observed in the magnetic vortex cores of the thin film sample with the double superconducting gaps, the highest T_c of $\sim$6.2 K, and the enlarged lattice constant of $\sim$3.4 Å [41].

V. CONCLUSION

Using first-principles calculations, we uncover that the QES affords a unique way of tuning the T_c of a whole class of bulk superconductors like β-Bi$_2$Pd, where the T_c is suppressed by pressure starting from the atmospheric pressure or a lower pressure and cannot be improved because of the inability of further decreasing external pressure experimentally. The T_c of bulk β-Bi$_2$Pd can be suppressed/improved by hole/electron doping via a tensile/compressive QES without inducing phase transition. The tunable T_c stems from the competition between the Debye temperature and EPC, due to the QES-modified phonon frequency ω and N_F. Our findings not only provide an effective way of tuning the SC of bulk β-Bi$_2$Pd, especially of enhancing the T_c by QES induced effective "*negative*" pressure, which is otherwise impossible in the experiments of applying external pressure, but also are useful for understanding the experimentally reported variations of T_c in bulk β-Bi$_2$Pd and in the epitaxial β-Bi$_2$Pd thin film. The suppressing effects of the pressure and the hole-type substitution on SC can be explained by the unified theoretical framework of QES tuning T_c. In-plane tensile strains may provide a feasible route of further improving the T_c of the β-Bi$_2$Pd thin film. We believe the effect of QES exists widely in other superconductors.

[1] J. Bardeen, L. N. Cooper, and J. R. Schrieffer, Phys. Rev. **108**, 1175 (1957).

[2] A. Schilling, M. Cantoni, J. D. Guo, and H. R. Ott, Nature (London) **363**, 56 (1993).

[3] B. Keimer, S. A. Kivelson, M. R. Norman, S. Uchida, and J. Zaanen, Nature (London) **518**, 179 (2015).

[4] N. W. Ashcroft, Phys. Rev. Lett. **21**, 1748 (1968).

[5] J. M. McMahon and D. M. Ceperley, Phys. Rev. B **84**, 144515 (2011).

[6] M. Borinaga, I. Errea, M. Calandra, F. Mauri, and A. Bergara, Phys. Rev. B **93**, 174308 (2016).

[7] R. P. Dias and I. F. Silvera, Science **355**, 715 (2017).

[8] W. L. McMillan, Phys. Rev. **167**, 331 (1968).

[9] P. B. Allen and R. C. Dynes, Phys. Rev. B **12**, 905 (1975).

[10] V. V. Struzhkin, R. J. Hemley, H.-k. Mao, and Y. A. Timofeev, Nature (London) **390**, 382 (1997).

[11] A. P. Drozdov, M. I. Eremets, I. A. Troyan, V. Ksenofontov, and S. I. Shylin, Nature (London) **525**, 73 (2015).

[12] A. P. Drozdov, P. P. Kong, V. S. Minkov, S. P. Besedin, M. A. Kuzovnikov, S. Mozaffari, L. Balicas, F. F. Balakirev, D. E. Graf, V. B. Prakapenka *et al.*, Nature (London) **569**, 528 (2019).

[13] M. Somayazulu, M. Ahart, A. K. Mishra, Z. M. Geballe, M. Baldini, Y. Meng, V. V. Struzhkin, and R. J. Hemley, Phys. Rev. Lett. **122**, 027001 (2019).

[14] B. Lorenz and C. W. Chu, in *Frontiers in Superconducting Materials*, edited by A. V. Narlikar (Springer, Berlin, 2005), pp. 459.

[15] C. W. Chu, P. H. Hor, J. G. Lin, Q. Xiong, Z. J. Huang, R. L. Meng, Y. Y. Xue, and Y. C. Jean, in *Frontiers of High-Pressure Research*, edited by H. D. Hochheimer and R. D. Etters (Springer US, Boston, MA, 1991), pp. 383.

[16] L. Gao, Y. Y. Xue, F. Chen, Q. Xiong, R. L. Meng, D. Ramirez, C. W. Chu, J. H. Eggert, and H. K. Mao, Phys. Rev. B **50**, 4260 (1994).

[17] S. Margadonna, Y. Takabayashi, Y. Ohishi, Y. Mizuguchi, Y. Takano, T. Kagayama, T. Nakagawa, M. Takata, and K. Prassides, Phys. Rev. B **80**, 064506 (2009).

[18] Q. Liu, X. Yu, X. Wang, Z. Deng, Y. Lv, J. Zhu, S. Zhang, H. Liu, W. Yang, L. Wang *et al.*, J. Am. Chem. Soc. **133**, 7892 (2011).

[19] K. Igawa, H. Okada, H. Takahashi, S. Matsuishi, Y. Kamihara, M. Hirano, H. Hosono, K. Matsubayashi, and Y. Uwatoko, J. Phys. Soc. Jpn. **78**, 025001 (2009).

[20] H. Okada, K. Igawa, H. Takahashi, Y. Kamihara, M. Hirano, H. Hosono, K. Matsubayashi, and Y. Uwatoko, J. Phys. Soc. Jpn. **77**, 113712 (2008).

[21] X.-C. Pan, X. Chen, H. Liu, Y. Feng, Z. Wei, Y. Zhou, Z. Chi, L. Pi, F. Yen, F. Song *et al.*, Nat. Commun. **6**, 7805 (2015).

[22] D. Kang, Y. Zhou, W. Yi, C. Yang, J. Guo, Y. Shi, S. Zhang, Z. Wang, C. Zhang, S. Jiang *et al.*, Nat. Commun. **6**, 7804 (2015).

[23] L. D. Jennings and C. A. Swenson, Phys. Rev. **112**, 31 (1958).

[24] T. F. Smith and C. W. Chu, Phys. Rev. **159**, 353 (1967).

[25] B. Lorenz, R. L. Meng, and C. W. Chu, Phys. Rev. B **64**, 012507 (2001).

[26] S. J. Zhang, X. C. Wang, R. Sammynaiken, J. S. Tse, L. X. Yang, Z. Li, Q. Q. Liu, S. Desgreniers, Y. Yao, H. Z. Liu, and C. Q. Jin, Phys. Rev. B **80**, 014506 (2009).

[27] W. Yi, L. Sun, Z. Ren, W. Lu, X. Dong, H.-J. Zhang, X. Dai, Z. Fang, Z. Li, G. Che *et al.*, Europhys. Lett. **83**, 57002 (2008).

[28] N. Môri, H. Takahashi, Y. Shimakawa, T. Manako, and Y. Kubo, J. Phys. Soc. Jpn. **59**, 3839 (1990).

[29] K. Zhao, B. Lv, Y.-Y. Xue, X.-Y. Zhu, L. Z. Deng, Z. Wu, and C. W. Chu, Phys. Rev. B **92**, 174404 (2015).

[30] G. Pristáš, M. Orendáč, S. Gabáni, J. Kačmarčík, E. Gažo, Z. Pribulová, A. Correa-Orellana, E. Herrera, H. Suderow, and P. Samuely, Phys. Rev. B **97**, 134505 (2018).

[31] Y. Zhou, X. Chen, C. An, Y. Zhou, L. Ling, J. Yang, C. Chen, L. Zhang, M. Tian, Z. Zhang, and Z. Yang, Phys. Rev. B **99**, 054501 (2019).

[32] H. Hu, M. Liu, Z. F. Wang, J. Zhu, D. Wu, H. Ding, Z. Liu, and F. Liu, Phys. Rev. Lett. **109**, 055501 (2012).

[33] X. Zhang, P. Sharma, and H. T. Johnson, Phys. Rev. B **75**, 155319 (2007).

[34] D. Flötotto, Z. Wang, L. P. H. Jeurgens, and E. J. Mittemeijer, Phys. Rev. Lett. **109**, 045501 (2012).

[35] Z. Chen, R. Wu, M. Liu, H. Wang, H. Xu, Y. Guo, Y. Song, F. Fang, X. Yu, and D. Sun, Adv. Funct. Mater. **27**, 1702046 (2017).

[36] R. K. Raman, Y. Murooka, C.-Y. Ruan, T. Yang, S. Berber, and D. Tománek, Phys. Rev. Lett. **101**, 077401 (2008).

[37] J. Kanasaki, E. Inami, K. Tanimura, H. Ohnishi, and K. Nasu, Phys. Rev. Lett. **102**, 087402 (2009).

[38] M. Liu, Y. Han, L. Tang, J.-F. Jia, Q.-K. Xue, and F. Liu, Phys. Rev. B **86**, 125427 (2012).

[39] C. Si, W. Duan, Z. Liu, and F. Liu, Phys. Rev. Lett. **109**, 226802 (2012).

[40] Z. Wang and F. Liu, Sci. China-Phys. Mech. Astron. **60**, 026811 (2016).

[41] Y.-F. Lv, W.-L. Wang, Y.-M. Zhang, H. Ding, W. Li, L. Wang, K. He, C.-L. Song, X.-C. Ma, and Q.-K. Xue, Sci. Bull. **62**, 852 (2017).

[42] P. Giannozzi, S. Baroni, N. Bonini, M. Calandra, R. Car, C. Cavazzoni, D. Ceresoli, G. L Chiarotti, M. Cococcioni, I. Dabo *et al.*, J. Phys.: Condens. Matter **21**, 395502 (2009).

[43] D. R. Hamann, Phys. Rev. B **88**, 085117 (2013).

[44] J. P. Perdew, K. Burke, and M. Ernzerhof, Phys. Rev. Lett. **77**, 3865 (1996).

[45] S. Baroni, S. de Gironcoli, A. Dal Corso, and P. Giannozzi, Rev. Mod. Phys. **73**, 515 (2001).

[46] G. Kresse and J. Furthmüller, Phys. Rev. B **54**, 11169 (1996).

[47] G. Kresse and J. Hafner, Phys. Rev. B **48**, 13115 (1993).

[48] J.-J. Zheng and E. R. Margine, Phys. Rev. B **95**, 014512 (2017).

[49] A. B. Migdal, Sov. Phys. JETP **7**, 996 (1958).

[50] G. M. Eliashberg, Sov. Phys. JETP **11**, 696 (1960).

[51] E. R. Margine and F. Giustino, Phys. Rev. B **87**, 024505 (2013).

[52] N. Marzari, A. A. Mostofi, J. R. Yates, I. Souza, and D. Vanderbilt, Rev. Mod. Phys. **84**, 1419 (2012).

[53] S. Poncé, E. R. Margine, C. Verdi, and F. Giustino, Comput. Phys. Commun. **209**, 116 (2016).

[54] A. A. Mostofi, J. R. Yates, Y.-S. Lee, I. Souza, D. Vanderbilt, and N. Marzari, Comput. Phys. Commun. **178**, 685 (2008).

[55] N. N. Zhuravlev, Sov. Phys. JETP **5**, 1064 (1957).

[56] S.-W. Kim, H.-J. Kim, F. Ming, Y. Jia, C. Zeng, J.-H. Cho, and Z. Zhang, Phys. Rev. B **91**, 174434 (2015).

[57] I. R. Shein and A. L. Ivanovskii, J. Supercond. Nov. Magn. **26**, 1 (2013).

[58] B. T. Wang and R. M. Elena, J. Phys.: Condens. Matter **29**, 325501 (2017).

[59] C. Wolverton and A. Zunger, Phys. Rev. B **52**, 8813 (1995).

[60] S. Piscanec, M. Lazzeri, F. Mauri, A. C. Ferrari, and J. Robertson, Phys. Rev. Lett. **93**, 185503 (2004).

[61] E. R. Margine and F. Giustino, Phys. Rev. B **90**, 014518 (2014).

[62] C. Si, Z. Liu, W. Duan, and F. Liu, Phys. Rev. Lett. **111**, 196802 (2013).

[63] J.-Y. Guan, L.-Y. Kong, L.-Q. Zhou, Y.-G. Zhong, H. Li, H.-J. Liu, C.-Y. Tang, D.-Y. Yan, F.-Z. Yang, Y.-B. Huang *et al.*, Sci. Bull. **64**, 1215 (2019).

[64] Y. Imai, F. Nabeshima, T. Yoshinaka, K. Miyatani, R. Kondo, S. Komiya, I. Tsukada, and A. Maeda, J. Phys. Soc. Jpn. **81**, 113708 (2012).

[65] L. Che, T. Le, C. Q. Xu, X. Z. Xing, Z. Shi, X. Xu, and X. Lu, Phys. Rev. B **94**, 024519 (2016).

[66] J. L. Olsen, K. Andres, and T. H. Geballe, Phys. Lett. A **26**, 239 (1968).

[67] R. E. Hodder, Phys. Rev. **180**, 530 (1969).

[68] I. Loa and K. Syassen, Solid State Commun. **118**, 279 (2001).

[69] E. A. Ekimov, V. A. Sidorov, E. D. Bauer, N. N. Mel'nik, N. J. Curro, J. D. Thompson, and S. M. Stishov, Nature (London) **428**, 542 (2004).

[70] F. Giustino, Jonathan R. Yates, I. Souza, M. L. Cohen, and G. Louie, Phys. Rev. Lett. **98**, 047005 (2007).

[71] R. A. Klemm, Physica C **514**, 86 (2015).

[72] R. P. Smith, T. E. Weller, C. A. Howard, M. P. M. Dean, K. C. Rahnejat, S. S. Saxena, and M. Ellerby, Physica C **514**, 50 (2015).

[73] M. Sakano, K. Okawa, M. Kanou, H. Sanjo, T. Okuda, T. Sasagawa, and K. Ishizaka, Nat. Commun. **6**, 8595 (2015).

[74] A. Okazaki and M. Kawaminami, Mater. Res. Bull. **8**, 545 (1973).

[75] W. X. Li, R. Zeng, L. Lu, and S. X. Dou, Physica C **470**, S629 (2010).

[76] L. Fu and C. L. Kane, Phys. Rev. Lett. **100**, 096407 (2008).

[77] E. Herrera, I. Guillamón, J. A. Galvis, A. Correa, A. Fente, R. F. Luccas, F. J. Mompean, M. García-Hernández, S. Vieira, J. P. Brison, and H. Suderow, Phys. Rev. B **92**, 054507 (2015).

[78] K. Iwaya, Y. Kohsaka, K. Okawa, T. Machida, M. S. Bahramy, T. Hanaguri, and T. Sasagawa, Nat. Commun. **8**, 976 (2017).